Advances in Molten Slags, Fluxes, and Salts: Proceedings of The 10th International Conference on Molten Slags, Fluxes and Salts (MOLTEN16)
Edited by: Ramana G. Reddy, Pinakin Chaubal, P. Chris Pistorius, and Uday Pal
TMS (The Minerals, Metals & Materials Society), 2016

KINETICS OF PHOSPHORUS MASS TRANSFER AND THE INTERFACIAL OXYGEN POTENTIAL FOR BLOATED METAL DROPLETS DURING OXYGEN STEELMAKING

Kezhuan Gu[1], Neslihan Dogan[1] and Kenneth S. Coley[1]

[1]McMaster Steel Research Centre
Department of Materials Science and Engineering
McMaster University
1280 Main Street West, Hamilton, Ontario, Canada, L8S 4L7
Phone: 905-525-9140 x24503
Email: coleyk@mcmaster.ca

Keywords: BOF, Reaction Kinetics, Dephosphorization, Mass transfer, Metal Droplets, Interfacial Oxygen Potential

Abstract

Knowledge of oxygen potential is crucial for better understanding of fundamentals of refining reactions kinetics within droplets during oxygen steelmaking. In this study, the changes in the phosphorus content of droplets were measured with time using X-ray fluoroscopy technique at 1853K. Specifically, the effects of sulfur content on dephosphorization kinetics of droplets were investigated during periods of intense decarburization. The experimental results showed that the droplets with low sulfur contents (0.007wt%, 0.011wt%) exhibit a lower minimum phosphorous level and an earlier and more significant reversion compared to those with high sulfur contents. The authors suggest that dephosphorisation rate and maximum partition are favored at lower CO evolution rates as well as lower amount of CO gas generation which result in a higher interfacial oxygen potential between slag and bloated droplets. Equating the rate of CO evolution with that of FeO mass transport allowed mass transfer coefficient of FeO to be calculated, which show that FeO mass transport in dense slag is faster than it is in foaming slag.

Introduction

Several researchers have studied aspects of droplet behavior relevant to steelmaking including, decarburization [1-6], droplet generation [7-16], size distribution [17-18] and residence time [19]. Other workers have developed models [20-23] and conducted plant trials [24-28], which consider the role of droplets in the overall steelmaking process. Previous work in the authors' laboratory [19] introduced the Bloated Droplet model, which has since been employed in an overall BOF model [20-21]. Convincing experimental evidence for bloated droplets has been reported by several researchers [5,6,29]. The current paper presents research on the interplay between dephosphorization and decarburization in bloated droplets. Dephosphorization of steel and hot metal has been studied extensively, important details relevant to the current work can be found in the following publications [30-33]. The importance of the interfacial oxygen potential is demonstrated by considering Equations 1, and 2. Equation 1 is written for rate is control by mass transport in the metal; subscripts b and i represent the bulk metal and the interface respectively,

k_m is the mass transfer coefficient for phosphorus, W_m is the mass of metal, A is the area of the slag-metal interface and ρ_m is the density of the metal. It is clear that $[\%P]_i$ has a strong influence on the driving force for dephosphorization. Similar equations may be written for mass transport in the slag and for mixed control.

$$-\frac{d[\%P]}{dt} = \frac{A}{W_m} k_m \rho_m ([\%P]_b - [\%P]_i) \qquad (1)$$

L_P, the partition coefficient for phosphorus is given by Equation 2, where (%P) represents phosphorus in the slag and [%P] represents phosphorus in the metal. The subscripts e and i indicate equilibrium and interface respectively, $C_{PO_4^{3-}}$ is the phosphate capacity of the slag,

$$L_P = \frac{(\%P)e}{[\%P]e} = \frac{(\%P)_i}{[\%P]_i} = \frac{C_{PO_4^{3-}} p_{O_2}^{5/4} f_P M_P}{K_P M_{PO_4^{3-}}} \qquad (2)$$

$f_P$is the activity coefficient for phosphorus in the metal M_P and $M_{PO_4^{3-}}$ are the molar mass of phosphorus and phosphate respectively, K_P is the equilibrium constant for the dissolution of phosphorus gas in steel and P_{O_2} is the partial pressure of oxygen, in this case at the slag metal interface. This last term is critical in determining the phosphorus partition at the interface. Researchers are divided on the reaction which controls the oxygen partial pressure. Wei et al [34] showed that the interfacial oxygen partial pressure varied between that in equilibrium with carbon in the metal and that in equilibrium with FeO in the slag. Monaghan et al [31] found that, the oxygen potential was controlled by iron oxide in the slag at low stirring whereas Wei et al found that high stirring rates favoured control by carbon in the metal. Wei proposed that the interfacial oxygen potential was set by the balance of supply by FeO in the slag and consumption by carbon in the metal. By encouraging CO nucleation, high stirring rates favour lower interfacial oxygen potentials. Gu et al [35] demonstrated that the foregoing analysis could be applied to dephosphorisation of bloated droplets. Previous work in the authors' laboratory [6] showed that CO nucleation is strongly affected by sulphur. Gu et al [35] used this observation, to determine the dephosphorization rate as a function of CO evolution rate. The current work is aimed at quantifying the relationship between CO evolution during droplet swelling and the interfacial oxygen potential which drives dephosphorization.

Experimental Procedure

The experimental setup and procedure have been described elsewhere [35]. All experiments employed a vertical tube furnace equipped with, X-ray imaging to observe swelling of droplets, and a pressure transducer to measure gas evolution. 25g of slag prepared by mixing of reagent grade Al_2O_3, CaO, SiO_2 and FeO was placed in a 45 mm diameter alumina crucible and held at temperature for one hour. An iron droplet containing 2.62%C, 0.088% P, ~ 50ppm oxygen and sulphur between 0.007% and 0.021% [36] was then added to the slag. Samples were quenched at different reaction times and taken for chemical analysis using Inductively Coupled Plasma. The slag composition for all experiments was 35wt%SiO_2, 32wt%CaO, 17wt%Al_2O_3 and 16wt%FeO.

Results

The change of phosphorous and droplet size as a function of time and droplet sulfur content is

shown in Figure 1. Figure 2(a) shows that CO generation rate goes through a maximum at about 0.017wt%S which is higher than the 0.011 wt%S previously reported by the authors [37]. This discrepancy is believed to be related to a change in the technique for making the droplets and a more detailed explanation is currently under investigation by the authors. Inspection of Figure 2(b) shows the total amount of CO generated increases with increasing droplet sulfur content although the amount of gas produced by 0.021wt%S droplets is only slightly higher than for 0.017wt%S. It is also noteworthy that in Figure 2(b) the duration of peak gas generation is 12s, 13s, 12s and 23s corresponding to droplets with 0.007wt%S, 0.011wt%S, 0.017wt%S and 0.021 wt%S. respectively. An elongated period of peak gas generation lowers the interfacial oxygen potential but increases the residence time. Comparing gas generation during the incubation period for all conditions reveals similar initial decarburization rates, around 8.0E-6 mole/s.

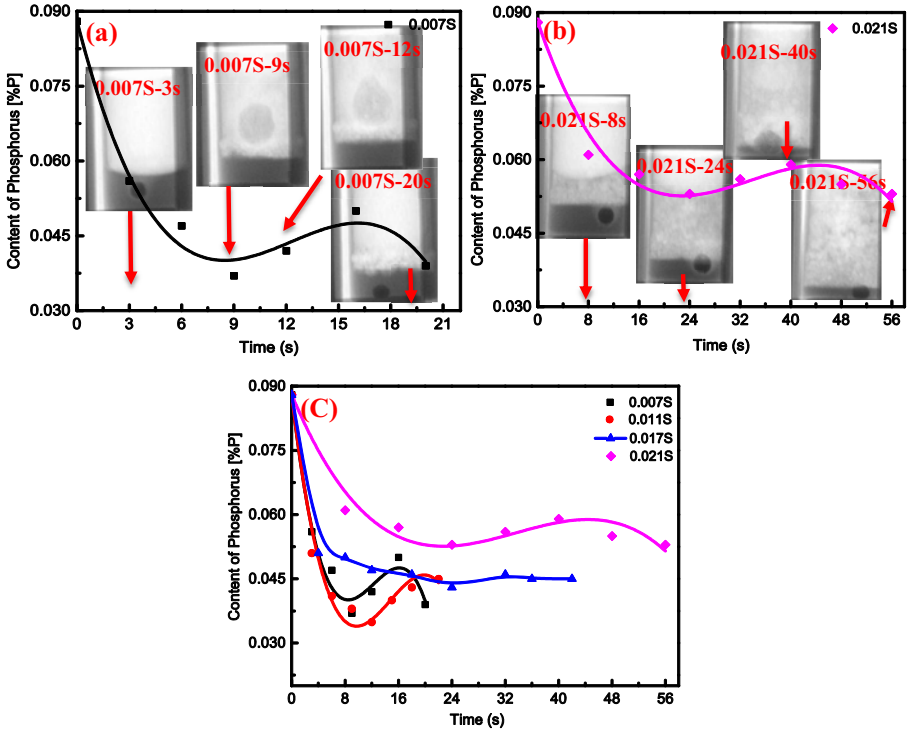

Figure 1: Plot of dephosphorization as a function of time and droplet sulfur content at 1853K: (a) 0.007wt%S; (b) 0.021wt%S and (C) all conditions.

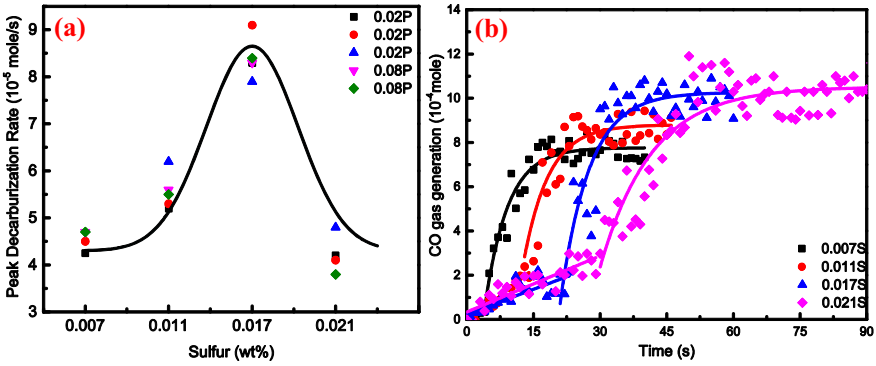

Figure 2: (a) CO evolution rate as a function of metal sulfur content at 1853K and (b) CO gas generation with time.

Comparing the data in Figure 1 with that in Figure 2 for droplets with sulfur less than 0.021, the phosphorus content at the reversion point is seen to increase with increasing CO evolution rate which is consistent with the authors' previous work [35]. However, the phosphorus concentration at the reversion point for 0.021wt%S droplets is much higher than 0.007wt%S droplets although they have a similar peak CO generation rate, and is higher compared to 0.017wt%S droplet which has the highest CO generation rate.

Inspection of the recorded X-ray videos reveals the time at which droplets float out of the dense slag as summarized in Figure 3(a). As the metal sulfur content increases, the time for droplets to float out of the dense slag increases to approximately 32 seconds for the 0.021 wt%S case. Figure 3(b) presents behaviors of droplets with different sulfur contents where droplets can be grouped according to behavior; those with lower sulfur contents (0.007wt%S and 0.011wt%S) have shorter incubation times and show similar behavior with regard to surface area change and dephosphorisation. For droplets with 0.017wt%S, they have the largest maximum surface area due to its' highest CO generation rate. Droplets with 0.021 wt%S have longest incubation time and despite the fact that they show similar decarburization rates to the droplets with 0.07wt%S the peak surface area is considerably lower. Defining the residence time as the time where droplet surface area is more than twice its original area, the peak width of each curve in Figure 3(b) is equivalent to residence time in the foam. Therefore, the residence times are approximately 11s, 14s, 16s and 22s for droplets with 0.007wt%S, 0.011wt%S, 0.017wt%S and 0.021 wt%S, respectively. Comparing results in Figure 1 with those in Figures 2 and 3, it is seen that the phosphorus content at the reversion point increases with increasing total amount of gas generation. The peak CO generation rate goes through a maximum with respect to sulfur which was suggested in previous work to be caused by the interplay between increasing rates of bubble nucleation and decreasing rates of growth with increasing sulfur [35]. Each of the two groups of droplets exhibit two distinct behaviors with respect to dephosphorization. The lower sulfur droplets exhibit a lower minimum phosphorous level and an earlier and more significant reversion. This behavior can be understood by considering the incubation time and the residence time in the foamy slag relative to the time for dephosphorisation. The low sulfur droplets

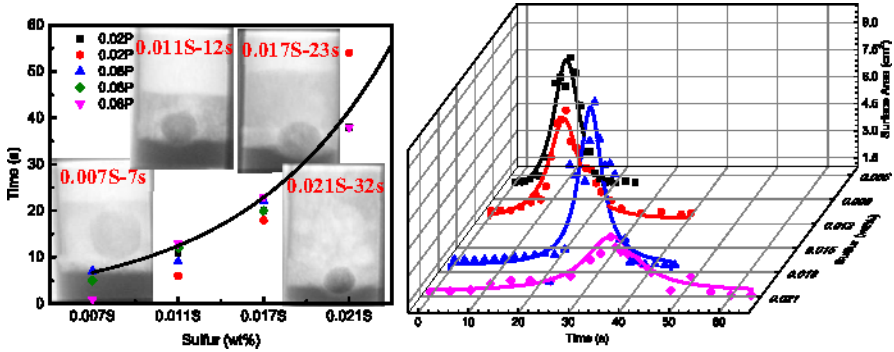

Figure 3: (a) Time needed for different droplets rise out of the dense slag and (b) Typical behavior of droplets with different metal sulfur content.

dephosphorized primarily in the dense slag and entered the foam shortly before reversion took place. The high sulfur droplets went through reversion before the droplet entered the foam. In the case of the low sulfur droplets approximately one third of the dephosphorisation occurred after the droplet entered the foam. The foam which is a much lower liquid slag volume than the dense slag will be quickly reduced driving phosphorous back into the metal. The high sulfur droplets do not swell and enter the foam until after reversion occurs. In this case the dephosphorization is slower probably because of a combination of a lower level of stirring in the metal and surface poisoning due to sulfur, the phosphorous that has been removed from the metal reverts to the slag when the carbon reaction accelerates leading to a lower oxygen potential at the slag-metal interface.

Figure 4(a) shows the volume of foaming slag as a function of time; the maximum volume is similar for all experiments at around 50 cm^3, five times higher than original dense slag (10cm^3). The rate of volume increase is tied to decarburization rate. The void fractions for different foaming slags are calculated and summarized in Figure 4(b). Here, void fraction for the whole residence time where droplets rest in foaming slag is calculated. As you can see, the average void fractions of 0.007%wtS and 0.011%wtS are 0.921 and 0.916 which is higher compared with 0.809 and 0.821 for 0.017wt%S and 0.021wt%S, respectively. The authors cannot offer an explanation for this observation but are investigating this phenomenon as part of ongoing research.

Discussion

The results presented above, show that dephosphorisation rate and maximum partition are favored at lower CO evolution rates as well as lower amount of CO gas generation which result

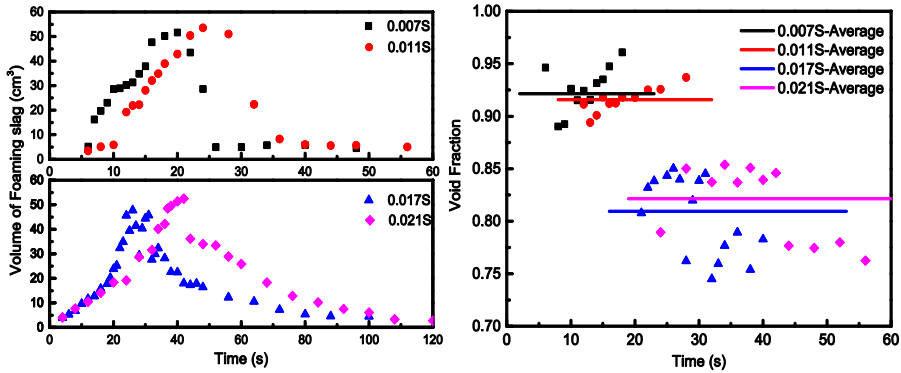

Figure 4: (a) The volume of foaming slag as a function of time and (b) Void fractions of foaming slag during droplet residence time in the foam

in a higher interfacial oxygen potential. These observations are consistent with the mechanism proposed by Wei et al [34] that the oxygen potential at the slag-metal interface is controlled by competition between oxygen supply from the slag and oxygen consumption by reaction with carbon in the metal, represented in this case by CO evolution rate. Based on this concept one can determine a dynamic interfacial oxygen potential by equating the rates of supply and consumption as shown in Equation 3.

$$k_{FeO}\left(C^{b}_{FeO} - C^{i}_{FeO}\right) = \frac{1}{A}\frac{dn_{CO}}{dt} \qquad (3)$$

Here, $\frac{dn_{CO}}{dt}$ is the CO generation rate (mol/s), C_{FeO} is the concentration of FeO, A is the surface area of the droplet, k_{FeO} is the mass transfer coefficient for FeO in the slag and superscripts b and i indicate bulk and interfacial values respectively. If C^{i}_{FeO} is expressed as activity of oxygen and the equation rearranged and C^{b}_{FeO} expressed as a function of the initial value C^{o}_{FeO} and the amount reduced, one obtains:

$$P^{i}_{O} = \left[\frac{\gamma_{FeO}K_{Fe}}{C*a^{i}_{Fe}*K_{O}}\left(C^{o}_{FeO} - \frac{1}{V_{dS}}\int\frac{dn_{CO}}{dt}dt - \frac{1}{A}\frac{1}{k_{FeO}}\frac{dn_{CO}}{dt}\right)\right]^{2} \qquad (4)$$

Where K_{Fe} and $K_{O}$are the equilibrium constants for FeO dissociation and oxygen dissolution in iron γ_{FeO} is the activity coefficient for FeO in the slag, C is the overall molar density of the slag, C^{o}_{FeO} is molar concentration of FeO in the slag and V_{dS} is the volume of dense slag. Although the CO evolution rate has been shown the dependence on CO nucleation, the authors are yet to develop a model which includes the bubble growth effect, therefore in the current work $\frac{dn_{CO}}{dt}$ has been determined empirically using pressure transducer data. From Figure 1 it is known that droplets experience phosphorus reversion in the foaming slag but obtain driving force to dephosphorize again when sinking back into the dense slag. This manifests that foam slag and dense slag have different mass transfer coefficient of FeO due to the difference of density.

Therefore, Equation 4 was modified to calculate the interfacial oxygen potential between foaming slag and bloating metal droplets when take the foaming slag into consideration:

$$P_O^i = \left[\frac{\gamma_{FeO}K_{Fe}}{C*a_{Fe}^i*K_O}\left(C_{FeO}^o - \frac{1}{V_{dS}}\int_0^{t_f}\frac{dn_{CO}}{dt}dt - \frac{1}{V_{fS}}\int_{t_f}^{t}\frac{dn_{CO}}{dt}dt - \frac{1}{A}\frac{1}{k_{FeO}}\frac{dn_{CO}}{dt}\right)\right]^2 \quad (5)$$

Where V_{fS} is the volume of foaming slag and t_f represents the time when droplets enter the foaming slag.

If one assumes dense slag and foaming slag have different mass transfer coefficient of FeO and which do not change with time; it is possible to determine the mass transfer coefficient of FeO for different slag based on a technique presented in a recent publication by the authors [35]. The minimum points in Figure 1 are of particular interest because the forward and backward reaction rates for dephosphorisation are equal but decarburization and FeO reduction continue. Therefore, one can assume the system is in equilibrium with regard to phosphorus and that bulk concentrations may be used to calculate L_P for the interface. If the phosphate capacity of the slag is known, it is then possible to calculate the interfacial oxygen potential from Equation 2. Substituting into Equation 4 and 5 allows k_{FeO} to be calculated. From Table I, we can see that

Table I – Calculated Interfacial Oxygen Potential and Mass Transfer Coefficient of FeO

Droplets	S	P^i_{O2} based on minimum [P]e	k_{FeO}(cm/s) of dense slag	k_{FeO}(cm/s) of foam slag
1	0.007	2.51E-12		0.0013
2	0.011	2.34E-12		0.0018
3	0.017	1.56E-12	0.0055	
4	0.021	9.65E-13	0.0044	

the calculated mass transfer coefficient of FeO in the dense slag is higher than that in the foaming slag. This result is to be expected if one considers the pathway for mass transfer to be through the liquid the cross sectional area of the path is dramatically reduced by the presence of bubbles. In the case of 0.017wt%S and 0.021wt%S, droplets sit between dense slag and foaming slag at the early step of phosphorus reversion. But for the simplicity of calculation, we assume that they sit inside dense slag at the period of phosphorus reversion.

Comparing k_{FeO} in foaming slag with k_{FeO} in dense slag, the magnitude of difference between the two is only moderate rather than vast as expected. The reason is that in foaming slag with intensive voids, the mass transfer will be hindered due to the limits of the transport pathway. However for droplets in dense slag without too much voids, we still will not expect a high mass transfer coefficient of FeO due to the formation of gas halo around droplets. The gas halo formed at the outside layer will block the mass transfer inside dense slag by acting as a barrier layer. In order to study the kinetics of dephosphorization, Equation 1 for mass transport control in the metal phase is integrated and expressed in Equation 6. In this case, the surface area A in

$$Ln\left[\frac{[\%P]_b-[\%P]_e}{[\%P]_o-[\%P]_e}\right]\left(\frac{[\%P]_o-[\%P]_e}{[\%P]_o}\right)\left(\frac{W_m}{\rho_m A}\right) = -k_m t \quad (6)$$

Setting C = $\left[\frac{[\%P]_b-[\%P]_e}{[\%P]_o-[\%P]_e}\right]$ and B=$\left(\frac{[\%P]_o-[\%P]_e}{[\%P]_o}\right)\left(\frac{W_m}{\rho_m A}\right)$ Equation 6 becomes B ln $C = kt$

As A in Equation 6 changes with time, a time averaged area must be used [36]. The data presented in Figure 1 are re-plotted in Figure 5 according to Equation 6. Differences in droplet chemistry do not allow a definitive conclusion that the mass transfer in metal phase is the rate-determining step. However, when the data are normalized for driving force, the mass transfer coefficient is very similar at the initial dephosphorization period for droplets with sulfur less than 0.021. But for droplets with 0.017wt%S, Figure 5 shows a lower mass transfer coefficient after about 4 seconds, probably due to a gas halo formed around droplets as shown in X-ray photos. The authors believe that at higher sulfur levels bubbles mainly form at the outer layer of droplets (external decarburization) at the beginning, leading to a lower rate of surface renewal and lower mass transfer coefficients. For this to be the case, the rate must be controlled by mass transport in the metal. Work is ongoing in the authors' laboratory to elucidate the true rate determining step.

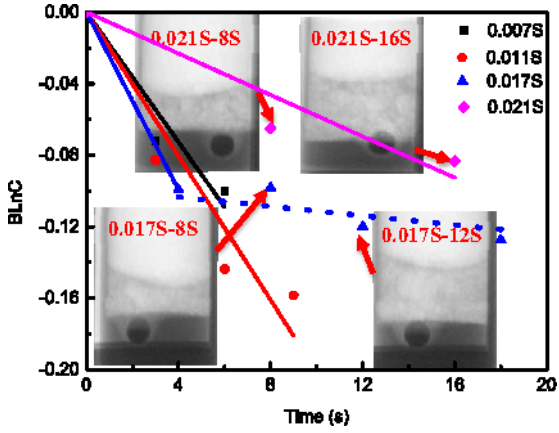

Figure 5: First order rate plot for dephosphorization as a function of metal sulfur content at 1853K

Conclusions

1. During dephosphorization of bloated liquid iron-carbon droplets the interfacial oxygen potential is controlled by the competition between supply of oxygen by iron oxide in the slag and consumption by formation of CO in the metal.

2. The phosphorus partition decreases with the increasing of metal sulfur content due to the increasing of total amount of CO gas, which lowers the interfacial oxygen potential.

3. Equating the rate of CO evolution with that of FeO mass transport allowed mass transfer coefficient of FeO to be calculated, which show that FeO mass transport in dense slag is faster than it is in foaming slag.

4. Internal decarburization offers a higher mass transfer coefficient due to the faster surface renewal rate, leading to a higher dephosphorization rate.

References

1. E.W. Mulholland, G.S.F. Hazeldean, and M.W. Davies, "Visualization Of Slag-Metal Reactions By X-Ray Fluoroscopy: Decarburization In Basic Oxygen Steelmaking," Journal of The Iron and Steel Institute, Vol. 211, September 1973, 632-639.
2.T. Gare and G.S.F. Hazeldean, "Basic Oxygen Steelmaking: Decarburization of Binary Fe-C Droplets and Ternary Fe-C-X Droplets in Ferruginous Slags," Ironmaking and Steelmaking, 1981, No. 4, 169-181.
3. H. Gaye and P.V. Riboud, "Oxidation Kinetics of Iron Alloy Drops in Oxidizing Slags," Metallurgical Transactions B, Vol. 8B, 1977, No. 9, 409-415.
4. D.J. Min and R.J. Fruehan, "Rate Of Reduction Of FeO In Slag By Fe-C Drops," Metall. Trans. B, 1992, vol. 23B, pp. 29-37.
5. C.L. Molloseau and R.J. Fruehan, "The Reaction Behavior of Fe-C-S Droplets In CaO-SiO2-MgO-FeO Slags," Metall. Trans. B, vol. 33B, 2002, pp. 335-344.
6. E Chen And K. S. Coley, "Kinetic Study of Droplet Swelling in BOF Steelmaking," Ironmaking And Steelmaking: Volume 37(7) October 2010, Pages 541-545
7. R.C. Urquhart and W.G. Davenport, "Foams and Dmulsions in Oxygen Steelmaking"Can. Metall. Quarterly, Vol. 12, No. 4, 1973, pp. 507-516.
8. N. Standish and Q.L. He, ISIJ Int., Vol. 29, No. 6, 1989, pp. 455-461.
9. Q.L. He and N. Standish, "A model study of droplet generation in the BOF steelmaking" ISIJ Int., Vol. 30, No. 4, 1990, pp. 305-309.
10. Q.L. He and N. Standish, "A model study of residence time of metal droplets in the slag in BOF steelmaking"ISIJ Int., Vol. 30, No. 5, 1990, pp. 356-361.
11. G. Turner and S. Jahanshahi, Trans. ISIJ, Vol. 27, 1987, pp. 734-739.
12. S.C. Koria and K.W. Lange, Ironmaking and Steelmaking, Vol. 10, No. 4, 1983, pp. 160-168.
13. S.C. Koria and K.W. Lange, "A new approach to investigate the drop size distribution in basic oxygen steelmaking",Metall. Trans., Vol. 15B, 1984, pp. 109-116.
14. S.C. Koria and K.W. Lange, "Estimation of drop sizes in impinging jet steelmaking processes", Ironmaking and Steelmaking, Vol. 13, No. 5, 1986, pp. 236-240.
15. Subagyo, G.A. Brooks, K.S. Coley, and G.A. Irons, "Generation of droplets in slag metal emulsion through top gas blowing", ISIJ Int., Vol. 43, No. 7, 2003, pp. 983-989.
16. Subagyo, G.A. Brooks, and K. Coley, "Interfacial area in top blown oxygen steelmaking", Steelmaking Conference Proceedings, ISS, Warrendale Pa., Vol. 85, 2002 pp. 749-762
17. Subagyo, G.A. Brooks, and K. Coley, "Residence time of metal droplets in slag metal gas emulsions through top gas blowing", Canadian Metallurgical Quarterly, Vol 44 [1], 2005, pp119-129
18. J. Schoop, W. Resch, and G. Mahn, Ironmaking and Steelmaking, Vol. 2, 1978, pp. 72-79.
19. G. A. Brooks, Y. Pan, Subagyo and K. S. Coley "Modeling of Trajectory and residence time of metal droplets in slag metal gas emulsions in oxygen steelmaking",Metall and Mater Trans B, Vol 36B, 2005, pp 525-535.
20. N. Dogan, G. A. Brooks And M. A. Rhamdhani, "Comprehensive Model of Oxygen Steelmaking Part I: Model Development and Validation," ISIJ International, 2011, Vol. 51, No. 7, pp. 1086–1092

21. N. Dogan, G. A. Brooks And M. A. Rhamdhani, “Comprehensive Model of Oxygen Steelmaking Part 2: Application of Bloated Droplet Theory for Decarburization in Emulsion Zone,” ISIJ International, 2011, Vol. 51, No. 7, pp. 1093–1101.
22. C. Kattenbelt and B. Roffel, “Dynamic Modeling of the Main Blow in Basic Oxygen Steelmaking Using Measured Step Responses,” Metall and Mater Trans B, 2008, vol 39B, pp764-769
23. R. sarkar, P Gupta, Somnath Basu, and Bharath Ballal, “Dynamic Modeling of LD Converter Steelmaking: Reaction” Modeling Using Gibbs’ Free Energy Minimization”, Metallurgical and Materials Transactions B, Published On-line Jan 2015
24. C. Cicutti, M. Valdez, T. Perez, R. Donayo and J. Petroni, “Analysis of Slag Foaming During the Operation of an Industrial Converter,” Latin Am.Appl. Res., 32 (2002), 237.
25. D.J. Price, “L.D.Steelmaking: Significance of the emulsion in carbon removal”,Process Engineering of Pyrometallurgy, Edited by M.J. Jones, The Institution of Mining and Metallurgy, London, UK, 1974, pp. 8-15.
26. B. Trentini, Trans. Met. Soc. AIME, Vol. 242, 1968, pp. 2377-2388.
27. P. Kozakevitch, “Foams and Emulsions in Steelmaking”,JOM, Vol. 22, No. 7, 1969, pp. 57-68.
28. A. Chatterjee, N.O. Lindfors, and J.A. Wester, Ironmaking and Steelmaking, Vol. 3, No. 1, 1976, pp. 21-32.
29. Pomeroy M., Chen, E., Coley, K. S. and Brown, G., “Kinetic Study of Droplet Swelling in BOF Steelmaking” Proceedings of The 6th European Oxygen Steelmaking Conference, Stockholm Sweden, September 7-9th (2011), 141-151 38
30.S. Basu, A.-K. Lahiri and S. Seetharaman, Distribution of phosphorus and oxygen between liquid steel and basic oxygen steelmaking slagRevue de Métallurgie / Volume 106 / Issue 01 / January 2009, pp 21-26
31. B.J. Monaghan, R.J. Pomfret, and K.S. Coley, “The Kinetics of Dephosphorization of Carbon-Saturated Iron Using an Oxidizing Slag”, Metall and Mater Trans B, 29B (1998), 111-118.
32. P. Wei, M. Sano, M. Hirasawa, and K. Mori, “Kinetics Of Phosphorus Transfer Between Iron-Oxide Containing Slag And Molten Iron Of High-Carbon Concentration Under Ar-O2 Atmosphere”, ISIJ.Int., 33 (1993), 479-87.
33. Christopher P. Manning and Richard J. Fruehan, “The Rate of Phosphorus Reaction between Liquid Iron and Slag”, Metallurgical And Materials Transactions B, Volume 44B, February 2013, pp37-44.
34. P. Wei, M. Ohya, M. Sano, and K. Mori, “Estimation Of Slag Metal Interfacial Oxygen Potential In Phosphorus Reaction Between Fe(T)O Containing Slag And Molten Iron Of High-Carbon Concentration” ISIJ. Int., 33 (1993), 847-54.
35. K. Gu, B. Jamieson, N. Dogan and K. S. Coley, “Kinetics of Dephosphorisation and the Interfacial Oxygen Potential for Bloated Metal Droplets During Oxygen Steelmaking”, 2015 AISTech Conference Proceedings.
36. M.A.Rhamdhani, G.A.Brooks and K.S. Coley, “The Kinetics of Dephosphorization of Carbon-Saturated Iron Using an Oxidizing Slag”, Metall and Mater Trans B, 36B (2005), 219-227.
37. E Chen and K.S. Coley, Ironmaking and Steelmaking: Volume 37(7) October 2010, 541-545.